PHYSICAL REVIEW A VOLUME 18, NUMBER 2 AUGUST 1978

Viscosity model for gases in the transition regime

D. Moronta and M. García-Sucre

Instituto Venezolano de Investigaciones Científicas, Centro de Física, Apartado 1827, Caracas, Venezuela

(Received 7 November 1977)

We have studied a model of tangential viscosity of a fluid in which high-order spatial derivatives of the velocity are taken into account. The model indicates that for a gas in the transition regime, and within a range of boundary conditions, the tangential stress presents an oscillatory dependence on the density. An experiment designed to detect these oscillations was done with helium at constant temperature $T = 294°K$ and varying the pressure within the range 0.5–50 mTorr. The results were found to be in good agreement with the oscillations predicted by our model when the spatial derivative of the fluid velocity near the boundaries was close to zero. From the separation in density between these oscillations, it is possible to obtain an independent measurement of the atomic mean cross section for helium. This method makes specific use of the way the viscosity oscillates with the density in the transition regime instead of using the value that the viscosity takes in the continuous regime. The good agreement between our measurements of the cross section and the values that have been obtained by other methods gives an indication of the validity of the proposed model.

I. INTRODUCTION

One of the main results of the kinetic theory of gases is that the viscosity is independent of the density in a range of pressures going approximately from 1 to $\frac{1}{60}$ atm.[1,2] For pressures less than $\frac{1}{60}$ atm, the viscosity measured at a constant temperature decreases with the pressure.[3-5] In regions of low pressures with a Knudsen number $K_n \gtrsim 1$, $K_n = l/L$, where l is the mean free path of the molecules of a gas and L is a characteristic length of the container, the viscosity goes to zero with the density.[6] The Knudsen regime $K_n > 1$ and the continuous regime ($K_n \ll 1$) are well known.[7] The intermediate-density region between these two regimes is sometimes called the transition regime. Cha and McCoy[8-10] have recently developed a transition-regime transport theory in rarified gases.

In the present paper we have studied the viscosity of a fluid in the transition regime following a somewhat different approach from that of Cha and McCoy in Refs. 8–10. A first rough approximation for the tangential stress P_{zx} is obtained making use of a Taylor-series expansion of the fluid velocity up to the third order in the spatial derivatives. A more-rigorous method is also used to obtain a relation of the same type for P_{zx} by solving the integral form of the Boltzmann equation in the relaxation-time approximation. This equation gives us a series of integrals in terms of the spatial derivatives of the velocity that can be exactly solved at least up to the one corresponding to the third order. The resulting equation for P_{zx} has a form similar to the one obtained by the Taylor-series method. However, the expressions for P_{zx} obtained by these two methods differ in the coefficient of the third-order term. These two expressions for P_{zx} also have a similar form to the one proposed by Cha and McCoy[8] who have solved the Krook equation[11] by the Chapman and Enskog method.[8,12] Although our treatment yields some of the results obtained by Cha and McCoy,[8] there are differences. For instance, the method we have used to solve the Krook equation (in its integral form) seems to us more straightforward and simple than the method used in Ref. 8. On the other hand, we have examined cases corresponding to boundary conditions which were not considered in Ref. 8. The experiment we have done with helium shows that the boundary conditions we have considered, which give rise in the transition regime to oscillations of P_{zx} as a function of the density, may occur in real systems. Furthermore, in Sec. IV, we will see how an independent determination of molecular diameters can be achieved from the oscillations of P_{zx} with the density. The molecular diameter for helium determined in this way is in good agreement with measurements performed using other methods.

II. THEORETICAL

A. Crude Taylor-series-expansion approximation to the problem

Let us consider an ideal gas located between two parallel surfaces separated by a distance L. Consider the lower surface at $z = 0$ fixed relative to the laboratory coordinates, and the upper one at $z = L$ moving along the axis x with a velocity u_M. Let us denote by P_{zx} the component of the stress tensor acting on the moving plate, and $u_x = u_x(z)$, the velocity of the layers of the fluid owing to the action of this plate. In the transition regime, i.e., $0.1 \lesssim K_n \lesssim 1$, the mean free path l of the molecules is large enough to consider high-order terms of a series expansion of the fluid velocity $u_x(z)$ about the point $l=0$:

$$u_x(z\pm l)=u_x(z)\pm\frac{\partial u_x}{\partial z}l+\frac{1}{2!}\frac{\partial^2 u_x}{\partial z^2}l^2 \pm\frac{1}{3!}\frac{\partial^3 u_x}{\partial z^3}l^3+\frac{1}{4!}\frac{\partial^4 u_x}{\partial z^4}l^4+\cdots . \qquad (1)$$

The mean force on a plane parallel to the plates and passing through the point z is due to the momentum transfer per unit area and unit time, and can be written approximately[13]

$$P_{zx}=\tfrac{1}{6}nm\bar{v}[u_x(z-l)-u_x(z+l)]. \qquad (2)$$

From Eqs. (1) and (2) and keeping terms up to third order, we obtain

$$P_{zx}=-\eta\frac{\partial u_x}{\partial z}-\gamma\frac{\partial^3 u_x}{\partial z^3}, \qquad (3)$$

with

$$\eta=\frac{1}{3}nm\bar{v}l\simeq\frac{1}{3\sqrt{2}}\frac{m\bar{v}}{\sigma} \qquad (4)$$

and

$$\gamma=\frac{1}{18}nm\bar{v}l^3\simeq\frac{1}{6\sqrt{2}}\frac{m\bar{v}}{\sigma^3 n^2}, \qquad (5)$$

where we have used the approximation $l\approx 1/\sqrt{2}\sigma n$ and the notations n, m, $\bar{v}$, and σ for the number of molecules per unit volume, mass of a molecule, mean molecular velocity, and the mean molecular cross section, respectively. Note that from Eqs. (1) and (2) it immediately follows that only the odd-order terms of the derivatives $\partial^m u_x/\partial z^m$ contribute. It should also be noted that in the linear term $-\eta\partial u_x/\partial z$ in Eq. (3) appears the well-known viscosity coefficient η which is independent of the density n. However, the coefficient γ appearing in Eq. (3) is density dependent, as is shown in Eq. (5).

B. Path-integral formulation

Consider now a less-crude model in which the distribution of molecular velocities is taken into account but the effects appearing in a detailed analysis of the collisions are neglected. For some of these effects this may be justified by the fact that we are concerned with rather low densities. In the path-integral formulation we have[14]

$$f(\vec{r},\vec{v},t)=\int_0^\infty\frac{f^{(0)}(\vec{r}_0(t'),\vec{v}_0(t'),t-t')e^{-t'/\tau}dt'}{\tau}, \qquad (6)$$

where $f(\vec{r},\vec{v},t)$ is the distribution function of the gas and, $f^{(0)}(\vec{r}_0(t'),\vec{v}_0(t'),t-t')$ is the complete time dependence of the Maxwell-distribution function for local equilibrium. The factor $e^{-t'/\tau}dt'/\tau$ is a collision probability, and τ is the average collision time that we will consider as constant.[13] We can write Eq. (6) in the following way:

$$f(\vec{r},\vec{v},t)=-\int_0^\infty f^{(0)}(\vec{r}_0(t'),\vec{v}_0(t'),t-t')\,de^{-t'/\tau}, \qquad (7)$$

which integrated by parts yields

$$f(\vec{r},\vec{v},t)=f^{(0)}(\vec{r},\vec{v},t)+\int_0^\infty\frac{df^{(0)}(\vec{r}_0(t'),\vec{v}_0(t'),t-t')}{dt'}\times e^{-t'/\tau}dt', \qquad (8)$$

where

$$f^{(0)}(\vec{r}_0(t'),\vec{v}_0(t'),t-t') =n\left(\frac{m\beta}{2\pi}\right)^{3/2}\exp\left(-\frac{\beta m}{2}[v_0(t')-u(r_0(t'),t-t')]^2\right) \qquad (9)$$

is a Maxwellian velocity distribution.

In the above expression $n=n(r_0(t'),t-t')$ and $\beta=\beta(r_0(t'),t-t')$ are the density and temperature parameters that we consider space and time independent. The fluid velocity $u(r_0(t'),t-t')$ is assumed to depend only on the z coordinate[13] [i.e., $u=u(z)$]. Furthermore, $v_0(t')=v(t_0)=v(t)$, where $t_0=t-t'$ since t' is a free-flight time in Eq. (9).

Introducing the definitions

$$U_x=v_x-u_x(z),\quad U_y=v_y,\quad U_z=v_z,$$
$$U=U_x\hat{x}+U_y\hat{y}+U_z\hat{z},$$

and

$$g(U_x,U_y,U_z)=n(m\beta/2\pi)^{3/2}e^{-(\beta m/2)U^2}, \qquad (10)$$

we can write

$$f^{(0)}(\vec{r},\vec{v},t)=g(U_x,U_y,U_z). \qquad (11)$$

The time dependence of $f^{(0)}(\vec{r}_0(t'),\vec{v}_0(t'),t-t')$ occurs only through the time dependence of the coordinate z in t'. This, together with $\vec{v}_0(t')=\vec{v}(t_0)$ and $t_0=t-t'$, allows us to write

$$\frac{df^{(0)}(\vec{r}_0(t'),\vec{v}_0(t'),t-t')}{dt'}=-\frac{df^{(0)}(\vec{z}(t_0),\vec{v}(t_0),t_0)}{dt_0}. \qquad (12)$$

From Eqs. (10)–(12) and the relations $dz(t_0)/dt_0=v_z(t_0)=v_z(t)$ and $U_x=v_x-u_x(z)$, we have

$$\frac{df^{(0)}}{dt'}=\frac{\partial g}{\partial U_x}\frac{\partial u_x(z)}{\partial z}v_z, \qquad (13)$$

which together with Eq. (8) yields

$$f(\vec{r},\vec{v},t)=g(U_x,U_y,U_z)+\int_0^\infty\frac{\partial g}{\partial U_x}\frac{\partial u_x}{\partial z}v_z e^{-t'/\tau}dt'. \qquad (14)$$

The integral I_1 that appears in the right-hand side of Eq. (14) can be integrated by parts:

$$I_1 = \frac{\partial g}{\partial U_x} \frac{\partial u_x}{\partial z} v_z \tau + \tau \int_0^\infty \left[\frac{\partial^2 g}{\partial U_x^2} \left(\frac{\partial u_x}{\partial z}\right)^2 v_z^2 - \frac{\partial g}{\partial U_x} \frac{\partial u_x}{\partial z^2} v_z^2 \right] e^{-t'/\tau} dt' . \tag{15}$$

Iterating the procedure, i.e., integrating by parts the integral appearing at each step, one gets an infinite series, which when inserted in Eq. (14) allows us to write

$$\begin{aligned} f(\vec{r},\vec{v},t) = {} & g(U_x,U_y,U_z) + \frac{\partial g}{\partial U_x} \frac{\partial u_x}{\partial z} v_z \tau + \frac{\partial^2 g}{\partial U_x^2} \left(\frac{\partial u_x}{\partial z}\right)^2 v_z^2 \tau^2 \\ & - \frac{\partial g}{\partial U_x} \frac{\partial^2 u_x}{\partial z^2} v_z^2 \tau^2 + \frac{\partial^3 g}{\partial U_x^3} \left(\frac{\partial u_x}{\partial z}\right)^3 v_z^3 \tau^3 + 3 \frac{\partial^2 g}{\partial U_x^2} \frac{\partial^2 u_x}{\partial z^2} \frac{\partial u_x}{\partial z} v_z^3 \tau^3 + \frac{\partial g}{\partial U_x} \frac{\partial^3 u_x}{\partial z^3} v_z^3 \tau^3 + \cdots . \end{aligned} \tag{16}$$

We will take all the terms of this series up to the one corresponding to the third order in the derivatives of $u_x(z)$, as was done in the Taylor-series development. The tangential stress P_{zx} in terms of the distribution function is given by[13]

$$P_{zx} = m \int d^3 v f(\vec{r},\vec{v},t) U_z U_x . \tag{17}$$

Inserting the value of $f(\vec{r},\vec{v},t)$ given by Eq. (16) in Eq. (17), we have

$$\begin{aligned} P_{zx} = {} & m \int d^3U \frac{\partial g}{\partial U_x} \frac{\partial u_x}{\partial z} v_z \tau U_z U_x + m \int d^3 U \frac{\partial^2 g}{\partial U_x^2} \left(\frac{\partial u_x}{\partial z}\right)^2 v_z^2 \tau^2 U_z U_x \\ & - m \int d^3U \frac{\partial g}{\partial U_x} \left(\frac{\partial^2 u_x}{\partial z^2}\right) v_z^2 \tau^2 U_z U_x + m \int d^3U \frac{\partial^3 g}{\partial U_x^3} \left(\frac{\partial u_x}{\partial z}\right)^3 v_z^3 \tau^3 U_z U_x \\ & + 3m \int d^3U \frac{\partial^2 g}{\partial U_x^2} \left(\frac{\partial^2 u_x}{\partial z^2} \frac{\partial u_x}{\partial z}\right) v_z^3 \tau^3 U_z U_x + m \int d^3U \frac{\partial g}{\partial U_x} \left(\frac{\partial^3 u_x}{\partial z^3}\right) v_z^3 \tau^3 U_z U_x + m \int d^3U g U_z U_x . \end{aligned} \tag{18}$$

Some of the integrals of Eq. (18) are zero by symmetry. The remaining integrals are

$$\begin{aligned} P_{zx} = {} & m \int d^3U \frac{\partial g}{\partial U_x} \frac{\partial u_x}{\partial z} v_z \tau U_z U_x \\ & + m \int d^3U \frac{\partial^3 g}{\partial U_x^3} \left(\frac{\partial u_x}{\partial z}\right)^3 v_z^3 \tau^3 U_z U_x \\ & + m \int d^3U \frac{\partial g}{\partial U_x} \left(\frac{\partial^3 u_x}{\partial z^3}\right) v_z^3 \tau^3 U_z U_x . \end{aligned} \tag{19}$$

The second integral of Eq. (19) gives rise to a sum of two identical terms with opposite signs that cancel out the value of the integral. Therefore, only the first and last integrals in Eqs. (19) do not cancel in our model. On the other hand, Cha and McCoy,[8,12] following a Chapman and Enskog method to solve the Krook equation, have found an equation essentially similar to Eq. (18). However, in their expansion occur nonlinear terms of power 3 in $\partial u_x/\partial z$ which do not exactly cancel. These terms were considered small and thus dropped out in their final expression (see, e.g., Ref. 8).

The solution of the first and third remaining integrals of Eq. (19) gives rise to

$$P_{zx} = -nkT\tau \left(\frac{\partial u_x}{\partial z}\right) - 3nm\tau^3 \left(\frac{kT}{m}\right)^2 \frac{\partial^3 u_x}{\partial z^3} , \tag{20}$$

which can be written

$$P_{zx} = -\eta \frac{\partial u_x}{\partial z} - \gamma \frac{\partial^3 u_x}{\partial z^3} \tag{21}$$

with

$$\eta = nkT\tau \simeq \tfrac{1}{3} nm\bar{v} l \tag{22}$$

and

$$\gamma = 3nm\tau^3 (kT/m)^2 \simeq \tfrac{1}{3} mn\bar{v} l^3 . \tag{23}$$

Equation (20) has the same form as Eq. (3) obtained by the Taylor-series expansion method. It should be noted, however, that the numerical coefficient for γ differs in both expressions, as can be seen in Eq. (5) and (23), which are, respectively, $\frac{1}{18}$ and $\frac{1}{3}$.

To introduce the boundary conditions, let us write Eq. (20) in the form

$$\frac{\partial^2 h(z)}{\partial z^2} + \omega^2 h(z) + \varphi = 0 , \tag{24}$$

where

$$\omega = (\eta/\gamma)^{1/2}, \tag{25}$$

$$\varphi = P_{zx}/\gamma, \tag{26}$$

and

$$h(z) = \frac{\partial u_x}{\partial z} . \tag{27}$$

The general solution to Eq. (24) is

$$h(z) = c_1 e^{i\omega z} + c_2 e^{-i\omega z} - P_{zx}/\eta . \tag{28}$$

From Eqs. (27) and (28) we can obtain a general solution to Eq. (20) or (21), which is

$$u_x(z) = \frac{c_1}{i\omega} e^{i\omega z} - \frac{c_2}{i\omega} e^{-i\omega z} - \frac{P_{zx}}{\eta} z + C_T . \tag{29}$$

The values $u_x(0)$ and $u_x(L)$ that $u_x(z)$ take at $z=0$ and $z=L$ are the fluid velocities just close to the fixed and moving solid surfaces, respectively. When slip occurs at the boundaries between the gas and the solid plates we have $u_x(0)>0$ and $u_x(L)<u_M$, where 0 and u_M are the velocities of the fixed and moving plates. In general, the slip increases monotonically as the density decreases, becoming pronounced when the mean free path is comparable to the separation between the solid surfaces.[15-17] An indication that slip occurs in the experiment discussed in Secs. III and IV is given by the drift of the experimental curve of the tangential stress (Fig. 4) towards lower values as the density decreases.

Let us introduce the boundary conditions $u_x(0)=u_0$ and $u_x(L)=u_L$, where u_0 and u_L are the fluid velocities just close to the fixed and moving solid surfaces for the specific system studied (if slip occurs we have $u_0>0$ and $u_L<u_M$). Separating the real and imaginary parts in Eq. (29), we have

$$u_x(z) = \left(u_L - u_0 + \frac{P_{zx}}{\eta} L\right) \frac{\sin(\omega z)}{\sin(\omega L)} - \frac{P_{zx}}{\eta} z + u_0 . \tag{30}$$

The other boundary condition that is necessary to specify is the derivative of the fluid velocity $u_x(z)$ just close to one of the plates. Thus we take

$$\left(\frac{\partial u_x(z)}{\partial z}\right)_{z=0} = a_0 . \tag{31}$$

The value of this derivative in the interphase gas-solid depends on the nature of the surface of the plate. Moreover, it depends on the way in which the molecules of the gas and the solid surface interact from a microscopic point of view.[18] Since it is very difficult to calculate a_0 for a particular system, we will study the tangential stress P_{zx} for different values of a_0. However, the following qualitative argument is an indication that the value of a_0 lies close to zero, as our experimental results tend to favor (Secs. III and IV). The argument is as follows: For $K_n \gtrsim 0.1$ the mean free path l of the gas molecules is macroscopic. We can choose a distance $\tilde{l}<l$ that is also macroscopic. From the definition of mean free path we can say that most of the molecules going close to the wall move with a uniform linear motion in the region of width $\tilde{l}$ just close to the wall. The same thing occurs for the molecules departing from the wall. In this way the mean value of the velocity of the molecules is approximately constant within this region. Therefore, we may expect that $\partial u_x/\partial z$ is close to zero for $0 \leqslant z \leqslant \tilde{l}$.

Note that the same argument can be used independently whether slip occurs or not at the solid surfaces. To see this, let us use the following simple model for the interaction of the molecules of the gas with the solid surfaces first introduced by Maxwell[19,20]: Let α be the coefficient of accommodation, i.e., the fraction of molecules that, after colliding with the solid surfaces, stick only to be reemitted afterwards with thermal velocity to the gas. Therefore, the fraction $1-\alpha$ corresponds to the molecules which are reflected specularly on the solid surfaces. The mean velocity $u_x(0)$ of the gas close to the fixed surface is approximately given by

$$u_x(0) \simeq 0\alpha + \left[u_x(0) + \left(\frac{\partial u_x(z)}{\partial z}\right)_{z=0} l + \frac{1}{2!}\left(\frac{\partial^2 u_x(z)}{\partial z^2}\right)_{z=0} l^2 + \frac{1}{3!}\left(\frac{\partial^3 u_x(z)}{\partial z^3}\right)_{z=0} l^3\right](1-\alpha) , \tag{32}$$

where we have made use of Eq. (1) up to the third order. The term 0α in Eq. (32) is the contribution to the mean velocity $u_x(0)$ coming from the molecules that stick to the surfaces and then are reemitted with thermal velocity. Since these molecules are generally assumed to be reemitted in a complete diffuse way, the mean value of the velocity component parallel to the surface of these molecules can be taken as equal to the velocity of the fixed surface, which we have fixed at zero. The second term on the right-hand side of Eq. (32) is the contribution coming from the molecules that are specularly reflected on the surface.

Since u_0 is the fluid velocity just close to the fixed surface, we can write from Eq. (32)

$$u_0 \simeq \frac{1-\alpha}{\alpha}\left[\left(\frac{\partial u_x(z)}{\partial z}\right)_{z=0} l + \frac{1}{2}\left(\frac{\partial^2 u_x}{\partial z^2}\right)_{z=0} l^2 + \frac{1}{6}\left(\frac{\partial^3 u_x}{\partial z^3}\right)_{z=0} l^3\right] , \tag{33}$$

the factor $s \equiv (1-\alpha)/\alpha$ appearing above is the usual slipping coefficient.[20] Note that when we take into account terms only up to the first order in Eq. (1), then Eq. (33) reduces to the well-known expression $u_0 \simeq sl(\partial u_x(z)/\partial z)_{z=0}$.[20]

From Eq. (33), it can be seen that there is no slip when $\alpha=1$, since in this case $s=0$ and $u_0=0$. On the other hand, when $\alpha<1$, slip occurs between the gas and the solid surface. We see now that, within this simple model of slipping, the qualitative consideration we have discussed above still favors that $a_0 \sim 0$ when slip occurs. Recall our argument that the molecules going close to the solid surface move with a uniform linear motion in this region of width $\tilde{l} < l$ just close to the surface. On the other hand, the same occurs for the molecules departing from the surface both in the case that these molecules are reemitted from the surface with thermal velocity and in the case that they are specularly reflected. Therefore, though the occurrence of slipping modifies the mean velocity $u_0 = u_x(0)$, again it may be expected that a_0 is around zero. The specific value that a_0 actually takes may be expected to depend on the nature of the solid surfaces (chemical composition and the surface finish), the kind of molecules of the gas, the number and velocity of the gas molecules colliding on the same surface element, and on the surface temperature.[18]

The region of the gas in the neighborhood of a solid surface of a width approximately equal to l is usually called the Knudsen layer.[21] Elaborate treatments of this region have been done. They consist essentially in solving approximately the Boltzmann equation in this region for a distribution function depending on a number of free parameters.[18,21] These free parameters depend in turn on the physical and chemical properties of the surfaces, the kind of incident molecules, the temperature of the gas and the solid surface, etc. Outside of the Knudsen layers, the validity of either the Navier-Stokes equations or the Burnett equations is assumed.[21] Furthermore, matching conditions are introduced at the boundaries between these two types of regions of the gas.[21] This way of taking into account the effect of the complex processes of interaction occurring at the gas-solid interphase on the whole gas presents a great deal of difficulty. Part of this comes from the scarce knowledge at the present time of the potential of interaction between the incident molecules and the molecules of the solid surface.[18,22]

However, calculations can be made within simplified versions of the above scheme. For instance, the case of weakly perturbed flows which correspond to a small relative velocity of the solid surfaces and a small temperature difference between these surfaces has been treated.[23] This has been done making use of a Krook equation[11] and simplifying assumptions on the interaction between the gas and the solid surfaces.[23] In the particular case in which there is no temperature difference between the solid surfaces, and accommodation factors are equal to unity, this yields a_0 smaller than $\Delta u/L$ ($\Delta u \equiv u_L - u_0$) for Knudsen numbers around unity.[23] Recall that $\Delta u/L$ is the value assumed for a_0 in the usual case of the continuous regime in which $l \ll L$.

This result points in the same direction as our qualitative consideration in favor of $a_0 \sim 0$. We will see below that according to our model an oscillatory behavior of P_{zx} as a function of n can occur if $a_0 \neq \Delta u/L$, which is a less restrictive condition than $a_0 = 0$. Yet, the oscillations of P_{zx} become more pronounced as $|a_0 - \Delta u/L|$ increases. On the other hand, our experimental results tend to favor that $a_0 < \Delta u/L$ (see Sec. IV). Also, the experiment we have done fulfills the conditions of weakly perturbed flows (see Sec. III and Ref. 23).

Deriving Eq. (30) with respect to z, and making use of the relation (31), we obtain

$$P_{zx} = -\eta \frac{\Delta u}{L} \frac{1 - (a_0/\Delta u)(\sin\omega L/\omega)}{1 - \sin\omega L/\omega L} = -\eta \frac{\Delta u}{L} f(n), \tag{34}$$

where $\Delta u = u_L - u_0$ and

$$\omega = (8/3\pi)^{1/2}\sqrt{2}n\sigma. \tag{35}$$

Equation (35) follows from Eq. (25) and the relations $l \approx 1/\sqrt{2}n\sigma$ and $\bar{v} = (8KT/\pi m)^{1/2}$. Figure 1 shows the value of P_{zx} given by Eq. (34) for different values of a_0.

It should be noted that Eq. (34) corresponds to a model in which P_{zx} is independent of z, and applies to a stable state in the sense that there are not any accelerated fluid layers. For this reason, specification of $u_x(0) = u_0$, $u_x(L) = u_L$, and a_0 determines completely the boundary conditions of the problem. On the other hand, we can see in Eqs. (34) and (35) that for the high-density limit, $n \to \infty$ corresponds to $\omega \to \infty$ and $\lim_{\omega \to \infty} P_{zx} = -\eta(\Delta u/L)$, which is the usual result (see Fig. 1). Furthermore, $P_{zx} = -\eta(\Delta u/L)$ is the correct expression for any density when the boundary conditions are so that $a_0 = \Delta u/L$. This last property gives a supple-

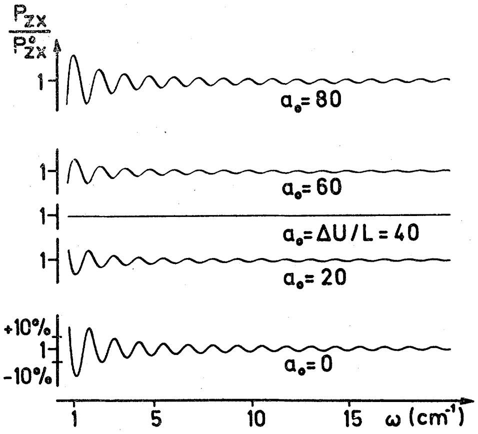

FIG. 1. Oscillations of P_{zx} for increasing ω for some values of a_0. $a_0 = \Delta u/L = 40$ sec^{-1} corresponds to the linear case, in which we have used $\Delta u = 200$ cm/sec and $L = 5$ cm.

mentary justification to the usual model in which $P_{zx} = -\eta(\Delta u/L)$ and $a_0 = \Delta u/L$. One of the assumptions in the usual simple model is that because $l \ll L$, the Taylor series given by Eq. (1) can be cut after the first-order term in l. However, as we have seen, this is not a necessary condition since with the boundary condition $a_0 = \Delta u/L$ we can use higher-order expansions and still retain $P_{zx} = -\eta(\Delta u/L)$.

When the boundary conditions are such that $a_0 \neq \Delta u/L$, the function P_{zx} given by Eq. (34) and shown in Fig. 1 oscillates with ω (and so with n) and with decreasing amplitude as n increases. When n is close to zero, then we are in a Knudsen regime and the model here described does not apply.

In connection with the oscillatory behavior that P_{zx} may present in the transition regime as a function of n, the question arises whether such oscillations could also occur for other transport phenomena such as heat conduction and diffusion. In favor of this possibility is the fact that for these transport phenomena we will have equations of the same form as Eq. (20).[24] In the case of heat conduction the heat flux and temperature take the place of P_{zx} and velocity. For diffusion the mass flux and the concentration take the place of P_{zx} and the velocity. However, according to what we have already seen, there are two types of requirements for the occurrence in the transition regime of the oscillations of P_{zx} as a function of n. These are, first, the structure of Eq. (20), and second, that boundary conditions are found in a certain range. An example illustrating this last point is provided by the fact that we have found that, in spite of Eq. (20), the oscillations of P_{zx} with n vanish when $a_0 = \Delta u/L$. In fact, for these oscillations to occur we must have $a_0 \neq \Delta u/L$, and they become sizable only when a_0 separates sufficiently from $\Delta u/L$ [see Eq. (34) and Fig. 1]. Therefore, it may be expected that also in the case of heat conduction and diffusion, boundary conditions play an essential role in the appearance of an oscillatory behavior as the n varies in the transition regime.[24]

The way to obtain experimentally boundary conditions favorable to the appearance of sizable oscillations may be different for each transport phenomenon. In the case of P_{zx} and heat conduction such a difference could be expected on the following grounds: (a) momentum and energy of the gas accommodate at different rates to the state of the solid surfaces, since in processes of interaction momentum transfer occurs much faster than energy exchange[22]; (b) in the exchange of energy between the gas and the solid boundaries, internal degrees of freedom of the gas molecules may be involved[25]; (c) exchange of energy by radiation between the gas and the solid boundaries contribute to the boundary conditions for heat conduction[25]; (d) in the case of heat conduction the density of the gas near one solid boundary is different from the density of the gas near the other boundary; (e) the temperatures of the two walls are different.

We have described in Sec. III an experiment to measure P_{zx} as a function of n in the transition regime. It seems that in the physical system with which the measurements have been done, the appropriate boundary conditions for observable oscillations of P_{zx} hold in the transition regime. It is our feeling that such oscillations could also occur for other transport processes in the transition regime provided that certain boundary conditions are obtained in the physical systems concerned. A pure phenomenological approach to this problem could be the searching of such boundary conditions by changing the chemical and physical nature of the solid boundaries, the temperature, and other parameters relevant to boundary conditions.[26] Another point is that measurement must be performed in such a way that the separation in density of the experimental points must be considerably shorter than the separation between the expected oscillations of the measured transport variable. If insufficient care is paid to this point, although the oscillations may be occurring, we will only observe a scattering of the experimental points in the transition-regime region of densities.

III. EXPERIMENTAL

A gas viscometer[27] was designed in order to make an experimental verification of the model of viscosity presented here. It consists basically of a cylindrical torsion pendulum of a large surface and low mass (see Fig. 2). A stainless-steel cylinder 120 cm long and 23.1 cm in diameter constitutes one of the fixed surfaces of the physical system. It is vacuum tight, and is the support of the peripheral instrumentation. An inner stainless-steel tube 100 cm long and 3.1 cm in diameter, located in the center, is the second fixed surface. Concentrically, and 5 cm from both fixed surfaces, there is a shell suspended from a 30-cm-long quartz fiber. This shell is made of aluminum-covered paper and is 78.1 cm long, 12.84 cm in diameter and weighs 58.63 g. An external torque can be applied to the fiber by means of a rotatory vacuum feedthrough, making the shell oscillate. The period of oscillation of the pendulum can be measured electronically with the aid of a laser beam reflected from a small mirror attached to the fiber.

The helium used for the experiment was purified

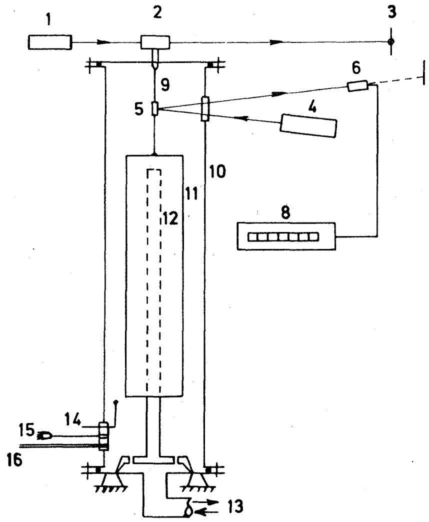

FIG. 2. Scheme of the experimental setting. 1, 2, and 3: laser, goniometer, and equilibrium center. 4, 5, and 6: laser, mirror and photocell, respectively. 7 and 8: screen and electronics for amplitude and period measurements. 9: quartz fiber. 10, 12: fixed surfaces. 11: moving surfaces (pendulum shell). 13: vacuum outlet and sample inlet. 14, 15, and 16: thermocouples and pressure gauges.

in a liquid nitrogen trap and its pressure, when in the viscometer, controlled to 1% in the range from 5 to 50 mTorr by a McLeod and by electrostatic pressure gauges. The working temperature was 294.1 ± 0.2 °K. The period of the pendulum is approximately 71 sec. A large period is desirable to avoid turbulence and to have good precision in the measurement of the period. Such measurements were made deflecting the pendulum 45°, and after 10 free oscillations a photocell placed in the path of the reflected light corresponding to the equilibrium position of the pendulum triggers a time-interval-measurement instrument in order to measure the time elapsed in 10 oscillations. For each period measurement the instrument was evacuated to 1 mTorr and then a new sample of helium was placed at the desired pressure.

The equation of motion of the pendulum is

$$I\ddot{\varphi} = -K\varphi - P_{zx}AR, \tag{36}$$

where I, φ, R, and A are the moment of inertia, deflection angle, the radius, and total surface of the oscillating shell, respectively. K is the torsion constant of the suspension. Since $I = MR^2$, where M is the mass of the pendulum, $\Delta u = \dot{\varphi}R$, and $P_{zx} = -\eta(\Delta u/L)f(n)$ [see Eq. (34)], we can write from Eq. (36)

$$\ddot{\varphi} + (1/\tau)\dot{\varphi} + 4\pi^2\nu^2\varphi = 0, \tag{37}$$

where

$$\nu \equiv (1/2\pi)(K/I)^{1/2} \tag{38}$$

and

$$1/\tau \equiv \eta f(n)(A/ML). \tag{39}$$

Note that L is the distance between the cylindrical shell and any of the fixed surfaces. The solution to Eq. (37) is the usual one given for a damped oscillator:

$$\varphi(t) = \varphi_0 e^{-\beta t}\cos(2\pi\nu t), \tag{40}$$

where

$$\beta = 1/2\tau = \eta f(n)(A/2ML) \tag{41}$$

and

$$\nu = (\nu_0^2 - \beta^2/4\pi^2)^{1/2}. \tag{42}$$

For our experimental setup in which $L = 5$ cm, we are interested in the range of pressures from 5×10^{-4} to 5×10^{-2} Torr. We will measure the periods T_i corresponding to the densities n_i in this range of pressures. Equation (42) relates the coefficient β with the frequencies $\nu_i = 1/T_i$. We take the frequency ν_0 appearing in Eq. (42) as equal to the frequency corresponding to the minimum value T_0 of the measured periods T_i (see Fig. 3).[28] We can write from Eqs. (41) and (42)

$$f(n) = \frac{4\pi ML}{\eta A}\,\frac{(T_i^2 - T_0^2)^{1/2}}{T_i T_0}. \tag{43}$$

Table I indicates different values T_i and the corresponding values of $f(n)$ for several pressures P_i. The minimum experimental value for the period was found to be 71.1172 ± 0.0002 sec, and for the value of the constant $4\pi ML/\eta A$ we used $M = 58.63 \pm 0.01$ g, $L = 5$ cm, $A = 6349 \pm 10$ cm^2, and $\eta = 194.1$ μP. This last value is the accepted one for the viscosity of He at 293 °K and normal pressure. To have an estimate of the error in the periods T_i, we

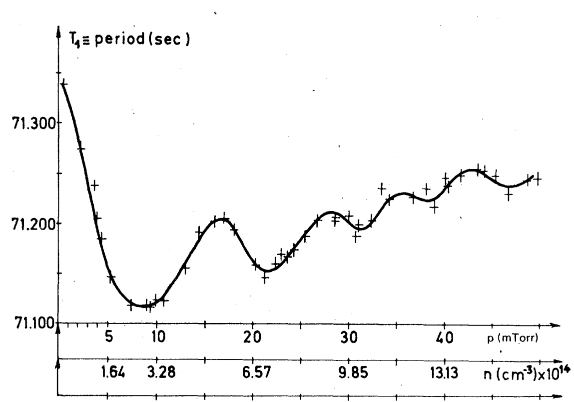

FIG. 3. Experimental values of the period T for different pressures. P, n, and l are pressure, density, and mean-free path, respectively.

performed several measurements at 21 °C and 17.1 mTorr. The standard deviation was found to be 0.0002 sec. On the other hand, since the overall temperature variation was 0.3 °C for the experiment, several measurements of the period T at 17.1 mTorr were made within a temperature range of 0.3 °C, and a standard deviation of 0.004 sec was obtained. The same was done for other points within the studied range of pressures, and essentially similar standard deviations were obtained. We have used the conservative value of 0.005 sec for the vertical error bars in Fig. 3. For the pressure, the horizontal error bars are 1 mTorr.

TABLE I. Measurements of the period of the pendulum and the function $f(n)$ given by Eq. (43), for helium at different pressures and $T = 294.1 \pm 0.2$ °K. The minimum value of the period, which was found at 9.2 ± 0.5 mTorr, was used as T_0 in Eq. (43). The error in the measurement of the pressure and period are ±0.5 mTorr and ±0.002 sec. The error for $f(n)$ is ±0.04.

Pressure (mTorr)	Period (sec)	$f(n)$
0.5	71.3395	3.3145
2.25	71.2741	2.7865
3.75	71.2386	2.4517
3.85	71.2041	2.0747
4.4	71.1830	1.8055
5.25	71.1446	1.1644
7.4	71.1181	0.2000
9.15	71.1181	0.2002
9.2	71.117295	0
9.85	71.1233	0.5462
10.9	71.1231	0.5370
13.0	71.1553	1.3735
14.35	71.1915	1.9185
16.0	71.2031	2.0628
17.2	71.2059	2.0961
18.1	71.1941	1.9518
20.25	71.1588	1.4353
21.15	71.1458	1.1897
22.2	71.1601	1.4576
22.9	71.1697	1.6126
23.6	71.1678	1.5832
24.25	71.1745	1.6848
25.45	71.1882	1.8755
26.75	71.2053	2.0890
28.4	71.2043	2.0771
28.55	71.2086	2.1278
30.0	71.2095	2.1382
30.7	71.1901	1.9004
31.0	71.2002	2.0277
32.3	71.2061	2.0985
33.3	71.2359	2.4244
34.2	71.2279	2.3414
36.5	71.2280	2.3424
38.0	71.2370	2.4356
38.9	71.2192	2.2476
39.9	71.2480	2.5447
40.3	71.2401	2.4668
41.6	71.2514	2.5775
43.2	71.2580	2.6400
44.0	71.2556	2.6175
45.25	71.2512	2.5756
46.75	71.2317	2.3812
49.75	71.2490	2.5544
50.6	71.2460	2.5252

In spite of the fact that we are interested in relative measurements instead of absolute ones, in order to check the apparatus reliability, we have done measurements of the absolute viscosity η in the continuous regime, in a range of pressures going from 1 to 400 Torr. To do this, a curved screen was used located at 2.10 m from the axis of the instrument. Following the motion of the reflected light from the mirror attached to the quartz fiber, the amplitude decrement of the pendulum was recorded. Table II shows the value of $\beta = (2.79 \pm 0.01) \times 10^{-3}$ sec.$^{-1}$ taken from the measured amplitude and the period $T = 71.973 \pm 0.005$ sec.

TABLE II. Measurement of the viscosity of helium at a pressure of 400 Torr and $T = 294.5 \pm 0.2$ °K by using the logarithmic amplitude decrement $\beta = (\ln A_0 - \ln A_N)/NT$, where T is the period of the pendulum and A_N is the amplitude of oscillation after N periods starting from the one corresponding to the amplitude A_0. The amplitudes were measured on a curved screen of radius equal to 210 cm and located at this distance from a small mirror on the quartz fiber of the pendulum. The error of the amplitudes measured on the screen is ±0.1 cm. The period of the pendulum in the above conditions is $T = 71.973 \pm 0.005$ sec. $\beta = (2.79 \pm 0.01) \times 10^{-3}$ sec^{-1} and the viscosity $\bar{\eta} = 259.6 \pm 0.5$ μp was obtained without taking into account geometric corrections (corrections arising because of ends, edges, defects of the walls, etc.), and slip factor corrections [see Eq. (41)].

N	A_N (cm)	$\beta \times 10^3$ (sec^{-1})
0	41.58	
0.5	37.68	2.737
1	33.95	2.816
1.5	30.88	2.756
2	27.70	2.822
2.5	25.30	2.761
3	22.62	2.820
3.5	20.70	2.769
4	18.5	2.813
4.5	16.90	2.780
5	15.19	2.798
5.5	13.81	2.784
6	12.41	2.800
6.5	11.32	2.781
7	10.12	2.805
7.5	9.25	2.784
8	8.22	2.815
8.5	7.60	2.778
9	6.79	2.797
9.5	6.18	2.788
10		

This gives a value for the viscosity of helium $\bar{\eta} = 2LM\beta/A$ of $\bar{\eta} = 259.6$ μP, without taking into account geometric and slip corrections. The geometrical corrections arise because of ends, edges, and defects of the walls, and the fact that we have neglected effects occurring because of the cylindrical symmetry of the system.[29] The absolute value of the viscosity of helium at 21 °C is 194.1 μP (see Sec. IV).

IV. DISCUSSION

Figures 3 and 4 show T and $f(n)$ as functions of n using the numerical values of the Table I. In the horizontal axes of these figures, the density is also expressed in terms of the mean free path l and the pressure. From the density interval Δn between two consecutive maxima or minima of the oscillatory shape of the curves, and making use of Eq. (35), it is possible to calculate the mean cross section of helium. Since the first two oscillations are the clearest, we take the experimental value $\Delta n = (3.94 \pm 0.65) \times 10^{14}$ molecules/cm^3. This corresponds to a pressure interval of 12 ± 2 mTorr and gives a value of $\sigma = (2.45 \pm 0.3) \times 10^{-15}$ cm^2 for He. Using the approximation $\sigma \simeq \pi d^2$, where d is the molecular diameter, we obtain for helium $d = (2.79 \pm 0.15) \times 10^{-8}$ cm. From tables,[30] the accepted values for d at 293 °K are $d_{tc} = 2.30 \times 10^{-8}$ cm, $d_{vw} = 2.65 \times 10^{-8}$ cm, and $d_v = 1.90 \times 10^{-8}$ cm, where d_{tc}, d_{vw}, and d_v are the molecular diameters calculated from thermal conductivity, Van der Waals excluded volume, and viscosity, respectively. Notice that our measurement of d is based on the way in which the viscosity oscillates with pressure in the transition regime instead of the constant value that the absolute viscosity has in the continuous regime as is done for the determination of d_v. Therefore, our determination of d is of a different nature than that corresponding to d_{tc}, d_{vw}, and d_v. The overall agreement between our value of d and d_{tc}, d_{vw}, and d_v is good. This is an indication that the oscillation of P_{zx} with decreasing pressures in the transition region detected in our experiment corresponds to a good measurement and gives reliability to the proposed model.

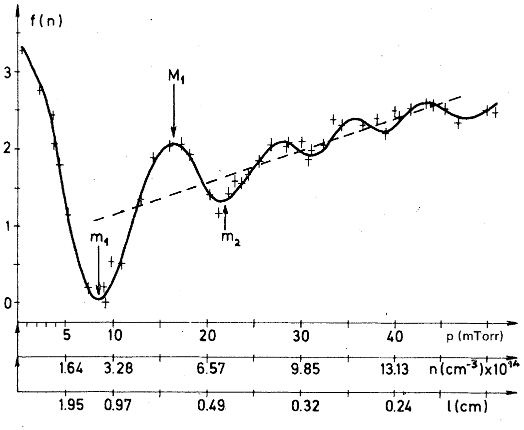

FIG. 4. Values of the function $f(n)$ calculated from Eq. (43) and the experimental values of the period of Table I.

Let us discuss now the problem of the value of a_0. If we compare Figs. 1 and 4 we see that despite the drift of the experimental curve appearing in Fig. 4 towards higher values of $f(n)$ as n increases, the shape of this curve corresponds to the shape of theoretical curves of Fig. 1 for a_0's smaller than $\Delta u/L$. Notice in Fig. 1 that for $a_0 < \Delta u/L$ the oscillations of $f(n)$ start at $f(n) > 1$ for n near to zero. This leads us to exclude $a_0 \geq \Delta u/L$, since in that case either the oscillations do not occur (when the equality stands) or the first oscillation starts with $f(n) < 1$ for n near to zero (see Fig. 1). Therefore, from the shape of the experimental curve of Fig. 4 we conclude that $a_0 < \Delta u/L$ for the system we have studied. Furthermore, the rather important values that the amplitude of oscillations shows in Fig. 4 is an indication that a_0 is noticeably different from $\Delta u/L$. This together with $a_0 < \Delta u/L$ ($\Delta u/L \simeq 0.03$ sec^{-1} in our experiment) makes it plausible that a_0 is close to zero.

We calculate now a_0 from the experimental curve of Fig. 4 and Eq. (43). The amplitude of oscillations of $f(n)$ depends strongly on the value of a_0. Systematic errors in the amplitude of oscillations have little influence on the separation Δn in density between maxima and/or minima of $f(n)$, which we have used to estimate the atomic cross section for helium. However, these errors may affect strongly the determination of a_0. There errors are essentially of two types. First, we have taken T_0 in Eq. (41) as equal to the minimum value of the measured periods, i.e., equal to the minimum of the curve appearing in Fig. 3. However, the true value of the period when there is no friction can be expected to be below the minimum of the curve represented in Fig. 3. Though we think that the true value T_0 is not far below the value we have actually used, this error will produce an overall vertical displacement of the curve in Fig. 4 together with a rather small deformation of the curve consisting essentially in flattening it. The region of the curve most modified by these changes will be that near to the minimum marked m_1 in Fig. 4 [see Eq. (43)]. To partially compensate for this type of error in the evaluation of a_0, we will use the $\Delta f(n)$ corresponding to the difference between the two extrema of $f(n)$ marked M_1 and m_2 in Fig. 4. M_1 and m_2 correspond to still quite clear oscillations of $f(n)$. Furthermore, M_1 and m_2 are consecutive extrema of $f(n)$, and thus the drift of $f(n)$ towards higher values as n increases will not perturb our measurement very much.

Another source of systematic errors is related to the fact that we have not taken into account geometric factors (corrections arising because of ends, edges, defects in the walls, etc.). This we have roughly compensated for by introducing the factor $\delta \equiv \eta/\tilde{\eta}$, where $\eta = 194.1\ \mu\mathrm{P}$ and $\tilde{\eta} = 259.6\ \mu\mathrm{P}$ are, respectively, the usually accepted value for the viscosity of He at $T = 293\,^\circ\mathrm{K}$ and the viscosity of He obtained with our instrument by measuring the logarithmic amplitude decrement β of the pendulum at 400 Torr and $T = 294\,^\circ\mathrm{K}$ (see Sec. III). This factor δ multiplies the factor ML/A in the equation for η if we obtain it from Eq. (41) by taking $f(n) = 1$ [note that $f(n) = 1$ for the conditions corresponding to the rather high density in which we have measured β]. Therefore $\delta = 0.75$ will appear multiplying Eq. (43). By measuring $\Delta f(n)$ in the experimental curve appearing in Fig. 4, multiplying it by 0.75, and calculating the difference between the two values of $f(n)$ corresponding to $\omega L = \frac{3}{2}\pi$ and $\omega L = \frac{5}{2}\pi$ in Eq. (34), we have obtained $a_0 = -0.03 \pm 0.04\ \mathrm{sec}^{-1}$. This crude determination of a_0 is consistent with $a_0 \sim 0$.

ACKNOWLEDGMENTS

We wish to thank R. Hausmann for the computational work and J. Serra for the drawings. This paper is based on a thesis submitted by one of us (D.M.) in partial fulfillment of the requirements for the Philosophus Scientarum in Physics degree at the Instituto Venezolano de Investigaciones Cientificas, 1977.

---

[1] J. C. Maxwell, Philos. Mag. January–July (1860).

[2] J. C. Maxwell, Philos. Trans. 156, 249 (1866).

[3] L. J. Stacy, Phys. Rev. 21, 239 (1923).

[4] K. S. Van Dyke, Phys. Rev. 21, 250 (1923).

[5] J. H. Jeans, *The Dynamical Theory of Gases*, 4th ed. (Dover, New York, 1954). Chap. XI, No. 374, and references therein.

[6] S. Chapman and T. G. Cowling, *The Mathematical Theory of Non-Uniform Gases* (Cambridge U.P., London, 1970), Chap. 6, No. 6-2, p. 100, and references therein.

[7] M. N. Kogan, *Rarified Gas Dynamics* (Plenum, New York, 1969), Sec. 4-2.

[8] C. Y. Cha and B. J. McCoy, J. Chem. Phys. 56, 3265 (1972).

[9] C. Y. Cha and B. J. McCoy, J. Chem. Phys. 56, 3273 (1972).

[10] B. J. McCoy and C. Y. Cha, Chem. Eng. Sci. 29, 381 (1974).

[11] P. L. Bhatnagar, E. P. Gross, and M. Krook, Phys. Rev. 94, 511 (1954).

[12] C. Y. Cha and B. J. McCoy, J. Chem. Phys. 54, 4369 (1971).

[13] F. Reif, *Fundamentals of Statistical and Thermal Physics* (McGraw-Hill, New York, 1965), Secs. 12 and 13.

[14] R. G. Chambers, Proc. Phys. Soc. Lond. A 65, 458 (1952).

[15] S. Chapman and T. G. Cowling, in Ref. 6, pp. 99–100.

[16] E. Bankenstein, Phys. Rev. 22, 582 (1923).

[17] R. S. Van Dyke, Phys. Rev. 21, 250 (1923).

[18] N. M. Kogan, in Ref. 7, pp. 88–99.

[19] J. C. Maxwell, Philos. Trans. R. Soc. I (1879); *The Scientific Papers of J. C. Maxwell* (Dover, New York, 1965).

[20] K. Huang, *Statistical Mechanics* (Wiley, New York, 1963), pp. 109–110.

[21] N. M. Kogan, in Ref. 7, Chap. V, and references therein.

[22] C. Cercignani, *Mathematical Methods in Kinetic Theory* (Plenum, New York, 1969), pp. 96–99.

[23] N.M. Kogan, in Ref. 7, pp. 298–315, see in particular Eq. (2.54) of p. 308 and Table 5 of p. 310.

[24] In the case of thermal conductivity, by following the same rough approach as was done for P_{zx} in Eqs. (1)–(5), we find similarly for the heat flux Q_z the relation

$$Q_z = -\tfrac{1}{3} nv \frac{\partial \epsilon}{\partial z} l - \tfrac{1}{18} nv \frac{\partial^3 \epsilon}{\partial z^3} l^3 ,$$

where ϵ is the mean energy per molecule. If we write this expression in terms of the temperature gradient, then

$$Q_z \simeq -\tfrac{1}{3} nvcl \frac{\partial T}{\partial z} - \tfrac{1}{18} nvl^3 \left[\frac{\partial^3 \epsilon}{\partial T^3} \left(\frac{\partial T}{\partial z} \right)^3 + 3 \frac{\partial^2 \epsilon}{\partial T^2} \frac{\partial T}{\partial z} \frac{\partial^2 T}{\partial z^2} + \frac{\partial \epsilon}{\partial T} \frac{\partial^3 T}{\partial z^3} \right],$$

where $c \equiv \partial \epsilon / \partial T$ is the specific heat per molecule. Assuming that c depends very slowly on the temperature, as is usually the case, then the above relation for Q_z reduces to

$$Q_z \simeq -\tfrac{1}{3} nvcl \frac{\partial T}{\partial z} - \tfrac{1}{18} nvcl^3 \frac{\partial^3 T}{\partial z^3} .$$

Then by following similar steps as in Eqs. (21)–(35) for the case of P_{zx}, we obtain

$$Q_z \simeq -k \frac{\Delta T}{L} \left(1 - \frac{b_0}{\Delta T} \frac{\sin \Omega L}{\Omega} \right) \Big/ 1 - \left(\frac{\sin \Omega L}{\Omega L} \right),$$

where k is the coefficient of thermal conductivity of the substance, $\Delta T = T(L) - T(0)$, $b_0 = (\partial T / \partial z)_{z=0}$ and $\Omega \simeq \sqrt{2} n \sigma$. Here again if b_0 is considerably different from $\Delta T/L$, oscillations of Q_z could become sizable, and the separation in density between the oscillations are the same as for the case of P_{zx}. However, in practice, the method to obtain boundary conditions such that $b_0 \neq \Delta T/L$ may be different from the method to obtain $a_0 \neq \Delta u/L$ in the case of P_{zx} (see the end of Sec. II). Note that the dependence of c on T for the gas far from the boundaries (c can be taken as independent of T in this region) may be different from that of the gas in the immediate neighborhood of a solid boundary. This may introduce an additional complication to the problem.

[25] J. P. Hartnett, *Rarified Gas Dynamics*, edited by L. Talbot (Academic, New York, 1961), Suppl. 1, pp. 1–28.

[26] This is quite an open question. We will study elsewhere the case of thermal conductivity by following a similar model to that we have used for P_{zx} in the present paper. In the experimental determinations we will try to work with physical systems in which a set of different boundary conditions could be obtained.

[27] D. Moronta (unpublished).

[28] The true period of the pendulum without friction [T_0 in Eq. (43)] can be expected to have a somewhat smaller value than the period corresponding to the minimum of the curve appearing in Fig. 3. Although we can neglect the friction produced by the fiber of quartz, there still remains some friction produced by the gas when densities are around the density corresponding to the minimum of the periods represented in Fig. 3. On the other hand, we could not eliminate this residual friction by producing an extreme Knudsen regime because of the limitations of our instrument. The Knudsen regime becomes predominant for pressures smaller than 1 mTorr in Fig. 3. Then it may be expected that when we approach zero pressure starting from 1 mTorr the period goes down to a value smaller than that of the lower period actually represented in this figure.

[29] E. Kearsley, *Transactions of the Society of Rheology* III, 69 (1959).

[30] *Handbook of Chemistry and Physics*, 52nd ed. (Chemical Rubber, Cleveland, 1971–1972), p. F–170.